Pertanika J. Sci. & Technol. 25 (1): 191 - 200 (2017)

SCIENCE & TECHNOLOGY

Journal homepage: http://www.pertanika.upm.edu.my/

Modelling the Effect of Sediment Coarseness on Local Scour at Wide Bridge Piers

Nordila, Ahmad[1]* Thamer, Mohammad[2], Melville, Bruce W.[3], Faisal, Ali[1] and Badronnisa, Yusuf[2]

[1]*Department of Civil Engineering, Faculty of Engineering, National Defence University of Malaysia, Kem Sungai Besi, 57000 Kuala Lumpur, Malaysia*

[2]*Department of Civil Engineering, Faculty of Engineering, Universiti Putra Malaysia, 43400 UPM, Serdang, Selangor, Malaysia*

[3]*Department of Civil and Environmental Engineering, University of Auckland, 20 Symonds St. Auckland1010, New Zealand*

ABSTRACT

Experimental data from a physical model of scouring around a cylindrical wide pier embedded in two types of uniform sediment beds are presented. The effects of sediment sizes and various pier widths on scour development and equilibrium scour depth of wide bridge piers are described. Existing literature suggest that the empirical scour prediction equations based on laboratory data over-predict scour depths for large structures. The present study has attempted to fill this gap for a cylindrical wide pier. Further, equations for the estimation of non-dimensional maximum scour depth for a wide cylindrical pier embedded in uniform sediment were proposed as functions of the sediment coarseness.

Keywords: Physical model, scour, wide piers, uniform sediment, sediment coarseness

INTRODUCTION

Many studies have been carried out with the objective of developing maximum scour depth for bridge piers. However, studies on measuring the scour depth for wide bridge piers are limited. By using laboratory and field data for large piers, a correction factor, K_w, was introduced for wide piers in shallow flows (Johnson & Torrico, (1994; Arneson et al. (2012)). A wide pier is defined as a pier which is located in a shallow channel with low-velocity flow, and y/b < 0.8 for Froude

Article history:
Received: 02 March 2016
Accepted: 14 December 2016

E-mail addresses:
nordila@upnm.edu.my; nordilaahmad1@gmail.com (Nordila, Ahmad),
thamer@upm.edu.my (Thamer, Mohammad),
b.melville@auckland.ac.nz (Melville, Bruce W.),
fahali@gmail.com (Faisal, Ali),
nisa@upm.edu.my (Badronnisa, Yusuf),
*Corresponding Author

ISSN: 0128-7680

number < 0.8 (Johnson, 1999) while Sheppard et al. (2011) noted that piers have a width to sediment diameter ratio greater than 100. Sheppard et al. (2004) and Lee and Sturm (2009) showed that parameter b/d_{50} or sediment coarseness has a significant impact on equilibrium local scour depth at wide piers. The predictive equations in the literature are intended for large and small piers (Sheppard et al. (2011)). Therefore, this situation leads to the over-prediction of local scour at such piers, thus, leading to the use of unwarranted and costly foundations or countermeasures. Therefore, local pier scour experiments were performed in the laboratory to investigate the effect of sediment coarseness (b/d_{50}) using two uniform sediment sizes and five bridge pier models. The equilibrium local scour depth at wide piers can be expressed by an empirical relation and is discussed here. The aim of this study is to show the relationship between dimensionless pier scour depth and the ratio of pier width to sediment size over a large range of physical scales.

METHODOLOGY

Experiments reported in this paper were conducted in a flume 50.0 m long, 1.5 m wide, and 2.0 m deep located at the Hydraulics Laboratory of the National Hydraulic Research Institute of Malaysia (NAHRIM), which contains a 0.4-m-deep sediment recess. A test area is located in the brick-sided part of the flume in the form of a recess, 10 m long, filled with uniform sediment of up to 0.4 m depth. The flow water depth was maintained at 0.25 m and the water discharged was controlled by an inlet valve. Cohesionless uniform sediments were used as bed material with median particle sizes of d_{50} = 0.23 and 0.80 mm and geometric standard deviations of σ_g = 1.3 and σ_g = 1.26 respectively. As shown in Table 1, five different pier diameters, 0.06, 0.076, 0.102, 0.140, and 0.165 m, were chosen for this study. The study was conducted under clear-water conditions at a threshold flow intensity of $U/U_c \cong 0.95$. U_c was estimated using the Shields Function proposed by Melville and Coleman (2000).

RESULTS AND DISCUSSION

Ten experiments were carried out. All of them were run for a single cylindrical pier with various diameters. Table 1 records the main parameters of the 10 experiments.

Table 1
Summary of experimental results for the present study

Pier	Velocity, U (m/s)	Critical velocity, U_c (m/s)	U/U_c	Time, t_e (h)	d_{50} (mm)	s_g	Diameter, b	d_s (m)
Pier 1	0.36	0.38	0.95	18	0.8	1.26	0.165	0.182
Pier 2	0.36	0.38	0.95	20	0.8	1.26	0.14	0.133
Pier 3	0.36	0.38	0.95	19	0.8	1.26	0.102	0.116
Pier 4	0.36	0.38	0.95	17	0.8	1.26	0.076	0.073
Pier 5	0.36	0.38	0.95	13	0.8	1.26	0.06	0.065
Pier 1	0.27	0.285	0.95	23	0.23	1.3	0.165	0.197
Pier 2	0.27	0.285	0.95	23	0.23	1.3	0.14	0.167
Pier 3	0.27	0.285	0.95	22	0.23	1.3	0.102	0.125
Pier 4	0.27	0.285	0.95	22	0.23	1.3	0.076	0.106
Pier 5	0.27	0.285	0.95	13	0.23	1.3	0.06	0.071

Scour Hole Development

The temporal development of local scour with a value of flow intensity U/U_c = 0.95 in a uniform sediment bed around a cylindrical pier is shown in Figure 1 (a)–(e). The plotted graphs show that the scour development can be divided into three stages: (i) the initial stage, (ii) the main erosion stage, and (iii) the equilibrium stage. The results are analysed based on the abovementioned stages of local scour development.

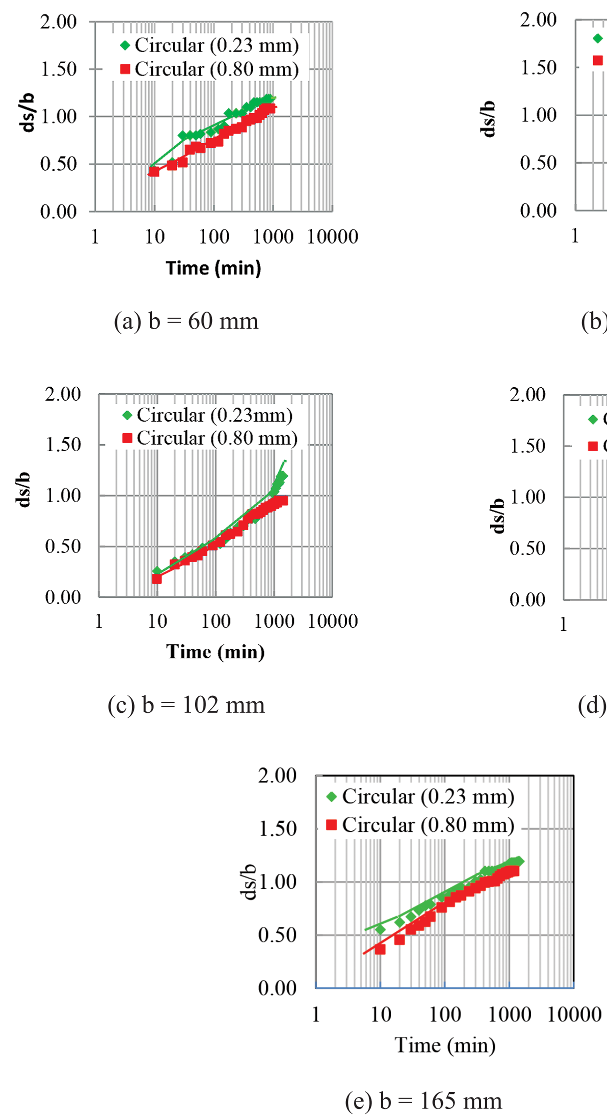

Figure 1. Normalised local scour depth (d_s/b) versus time at the same value of b in sediment beds of d_{50}=0.23 and 0.80 mm

Initial Stage. In each experiment, the local scour began on the plane bed immediately around the pier and at locations approximately ± 45° from the direction of flow. At these locations, a small depression is formed in the sediment at either side of the pier. The scouring begins where the local shear stress exceeds the critical value for the entrainment of bed particles. From the observation, once the grooves have formed in the sediment at the sides of the pier, the bed shear stress pattern around the pier changes. The downflow near the base of the pier was observed to be deflected to the sides of the pier by the pressure gradients. Overall, at this stage the maximum depths of scour at the pier are $d_s/b \approx 0.3$ and 0.39 at $d_{50} = 0.80$ and 0.23 mm, respectively.

Main Erosion Stage. In order to observe the zone within the scour hole influenced by the bed sediment, the parameter b/d_{50} is used. This parameter compares the scale of the secondary flow within the scour hole to the size of the bed particles. Ettema (1980) analysed the influence of bed sediment on equilibrium scour depth within the range b/d_{50} = 28–187. He classified the sediment as fine relative to the pier width when b/d_{50}> 130 and intermediate size when 130> $b/d_{50}{}^{3}$ 8. Since two sediments were used in this study, it is possible to identify two regions of sediment coarseness, b/d_{50}, in which either the development of scour differed or the equilibrium depth of scour diminished with increasing values of b/d_{50}. The scour development of these regions was also observed using two different sizes of bed sediment. The regions can be classified as (a) b/d_{50}> 230, with d_{50}=0.23 mm; and (b) b/d_{50}< 230, with d_{50}=0.80 mm. The development of local scour for values of the sediment coarseness, b/d_{50}, corresponding to regions (i) and (ii) are shown in Figure 2 (a)–(d) and 3 (a)–(d). Figure 4 gives a more definitive illustration of the development of local scour for values of b/d_{50} in the two regions (i) and (ii).

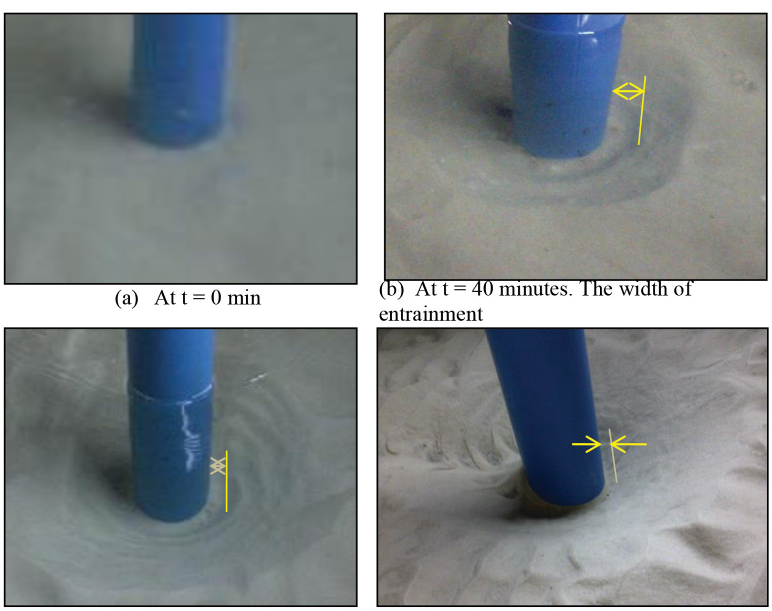

(a) At t = 0 min

(b) At t = 40 minutes. The width of entrainment

(c) t = 240 minutes. The width of entrainment zone at the pier nose is decreased

(d) t_e = 1440 minutes. The width of entrainment zone at the pier nose is

Figure 2. b = 140 mm, d_{50} = 0.23 mm, b/d_{50} = 609, U/U_c = 0.95

When b/d_{50}^{3} 230, the scour depth increases due to the strength of downflow in the vicinity of the pier nose. The downflow impinges on the base of the scour hole, eroding a nearly flat, narrow strip around the pier, and is deflected up the slopes of the scour hole to feed the horseshoe vortex. The measurement of the horseshoe vortex by Melville (1975) and observations of the motion of entrained sediment indicate that the entrainment zone corresponds to the contact area of the downflow impinging on the bed at the base of the scour hole with the underside of the horseshoe vortex on the slope of scour hole (Ettema et al., 2006). It is also observed that the erosion of sediment from the lower portion of the slopes in the scour hole disturbs the stability of the sediment so that it slides down into the entrainment zone each time the slope stabilises. Junliang and Xiong (2014) also added if the bed is erodible, such vortexes can enhance the transport of the sediment particles. The extent of the entrainment zone from the pier to about midway up the scour hole slope can be seen in Figure 2 (b). As the scour hole increases, the extent of the entrainment zone decreases until most of the sediment is entrained from the region in which the downflow near the pier impinges on the bed at the base of the scour hole. Ettema (1980) noted that from the depth of scour $d_s/b \approx 0.8$–0.9, the decrease in the extent of the entrainment zone indicates that the strength of the horseshoe vortex is decreasing. The photograph in Figure 2 (b)–(d) shows that the entrainment zone in this study decreases with time. An increasing strength of the horseshoe vortex from the flat bed ($d_s/b = 0$–9) followed by a decrease in the strength of the horse shoe vortex, was also observed in Melville (1975), where the author mentioned that the vortex expands in size but its rotational velocities decrease. Kirkil et al. (2008) also revealed the numerical solution where the interactions of the turbulences structures are particularly complex especially when the near wake region and horseshoe vortex system are merged. Figure 3 illustrates the scour process at b = 140 mm for a pier diameter placed in 0.80mm of bed sediment ($b/d_{50} = 175$). From the observations, at the beginning of the erosion stage the groove width increased to a value of approximately 0.11b, when the depth of scour was about $d_s/b \approx 0.5$, which is around t= 20–30 minutes for all pier sizes. As the scour depth increased to $d_s/b \approx 0.8$, the groove widened to approximately 0.24b and remained at this width until the equilibrium scour depth was attained for all pier sizes.

Equilibrium Stage. In uniform flow, the equilibrium scour depth is reached when the downflow impinging on the base of the scour hole is unable to erode particles from the scour hole. Figure 4 shows that the equilibrium scour depth decreased with increasing b/d_{50}. The curve indicates a high value of equilibrium scour depth achieved at $b/d_{50} = 330$ with b = 76 mm in fine sediment with $d_{50} = 0.23$ mm. The values of d_s/b for piers of 102, 140, and 165 mm show a little less than the peak value observed for the smaller piers at $d_{50} = 0.23$ mm.

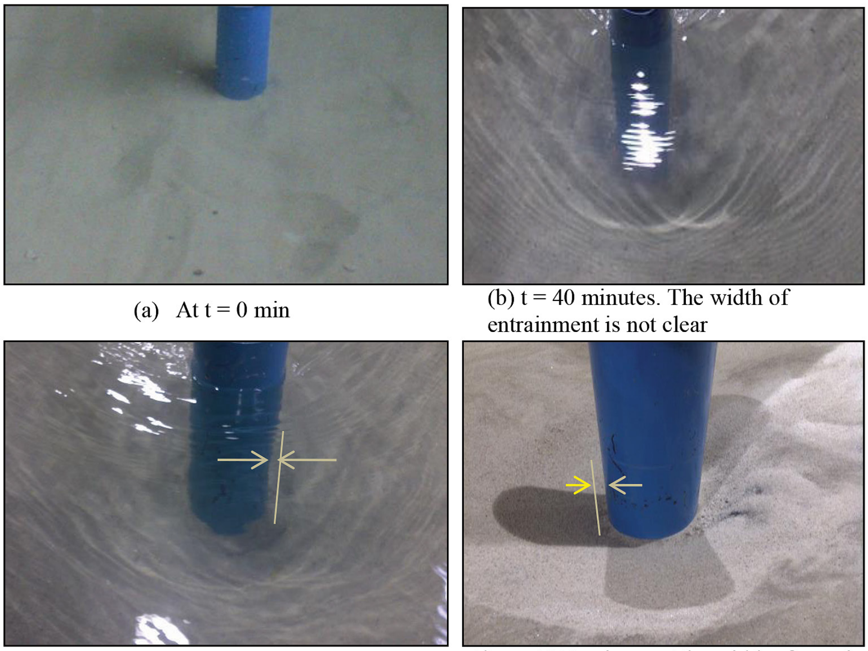

(a) At t = 0 min

(b) t = 40 minutes. The width of entrainment is not clear

(c) t = 240 minutes. The width of entrainment zone at pier nose is indicated

(d) t = 1320 minutes. The width of entrainment zone at the pier nose is indicated

Figure 3. b = 140 mm, d_{50} = 0.80 mm, b/d_{50} = 175, U/U_c = 0.95

The smaller maximum equilibrium scour depths recorded for the larger pier sizes may be due to the greater localised scour of the bed surface around the rim of the scour hole at each of these piers than for the smaller piers. Ettema (1980) noted that the reductions of scour depth for larger pier sizes were influenced by the adjustment of bed level at the upstream rim of the scour hole. This corresponds to the occurrence of a small rotation in bed level immediately upstream of the scour hole for larger piers (140 and 165mm) with regard to the main erosion stage. However, this upstream erosion was not observed with smaller piers in the same sediments. The equilibrium scour depth at two smaller piers was attained before the localised scour of the bed surface around the scour hole could affect the development of the scour at the pier. This phenomenon did not happen with the large piers, for which a considerably longer period of time was required to reach an equilibrium depth. However, all pier sizes for cases where the sediment is coarse relative to b (b/d_{50}< 230) show lower values compared with cases where the sediment is fine relative to b (b/d_{50}> 230) except at b/d_{50} = 608. These trends may occur because the downflow effect in the local scour process is higher in finer sediment which creates a deep hole in the vicinity of the pier base. Nicolet (1971) reported a similar peak of d_s/b at a pier diameter < 0.1 m and slightly lower equilibrium scour depths for larger pier sizes.

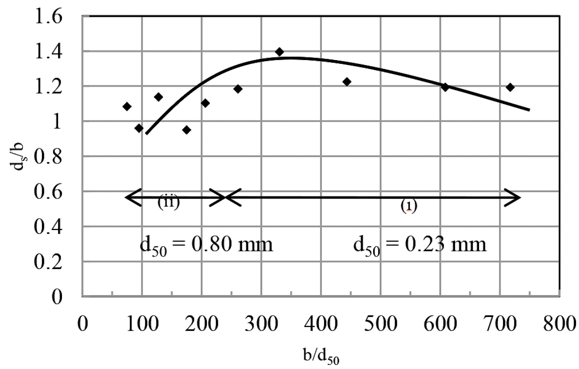

Figure 4. Equilibrium scour depth versus b/d_{50} for the present study

Effect of Sediment Coarseness

In order to demonstrate a wider range of applicability, laboratory data from the present study were merged with those obtained from other researchers. Figure 5 shows the equilibrium scour depth versus b/d_{50} for a large range of values of sediment coarseness. The continuous reduction in the dependence of d_s/b on b/d_{50} with increasing b/d_{50} differs from that noted by other researchers (Ettema, 1980; Jones & Sheppard, 2000; Sheppard & Miller, 2006; Lee & Sturm, 2009). The present study shows that the scour depth values were lower than those found by other researchers with a range of 0.95–1.39 and the maximum value of d_s/b occurred in ripple-forming sediment. Ettema (1980) showed that the range of maximum values of d_s/b in ripple-forming sediments with d_{50}< 0.7 mm were between 0.90 and 1.70. However, Rui et al. (2013) mentioned that the values was not so critical for sand bed d_{50} < 2mm and Melville (2008) showed that for a value of the shear velocity ratio U/U_c approaching unity or the threshold of motion condition for the bed sediment, a planar bed composed of fine sand can gradually develop ripples. This is because planar beds of ripple-forming sediments are unstable for bed shear stresses approaching the critical shear stress from particle entrainment. The formation of ripples on an initially planar bed surface increases the roughness of the bed and the mean bed shear stress, causing a low intensity of sediment transport into the scour hole. This could be the principal reason for the lower value of d_s/b indicated by this study compared with the findings of other researchers.

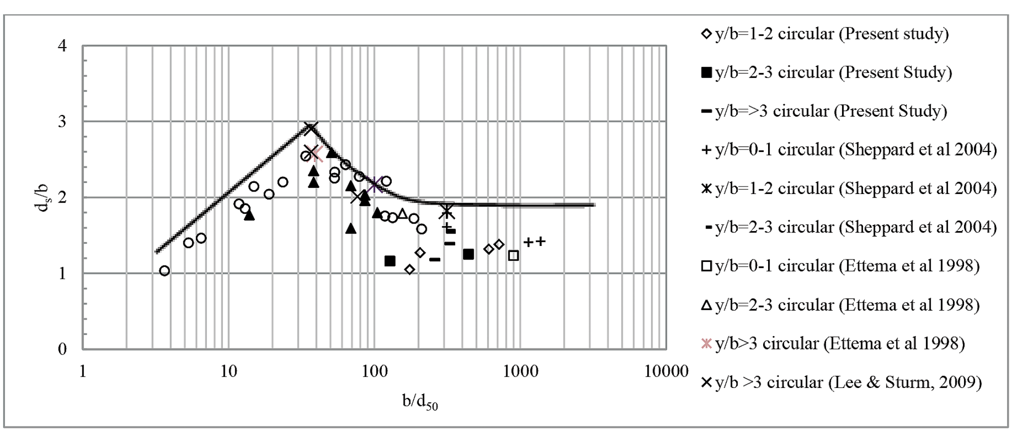

Figure 5. Effect of b/d_{50}on d_s/b

Data in Figure 5 are plotted as the upper envelope in the same figure and are represented by the following equation:

$$\frac{d_s}{b} = 0.05\left(\frac{b}{d_{50}}\right) + 1.11 \qquad 4 \le b/d_{50} \le 37 \qquad [1]$$

$$\frac{d_s}{b} = \frac{2}{\left(0.027\frac{b}{d_{50}} - 0.6\right)^{1.4} + 1.3} + 1.8 \qquad 37 \le b/d_{50} \le 1 \times 10^4 \qquad [2]$$

These plots also clearly show the reduced dependence of d_s/b on b/d_{50} with increased values of b/d_{50}, as mentioned by Sheppard et al., (2004); Lee and Sturm (2009); Rui et al., (2013) and Sheppard et al., (2014). All the values of the predicted d_s/b were compared with the values of the observed d_s/b obtained from the experimental work in this study and selected literature. Figure 6 compares d_s/b predicted with d_s/b observed using Equation [1] and [2]. It was demonstrated that values of d_s/b using Equation [1] and [2] are closer to the observed values with less under-prediction.

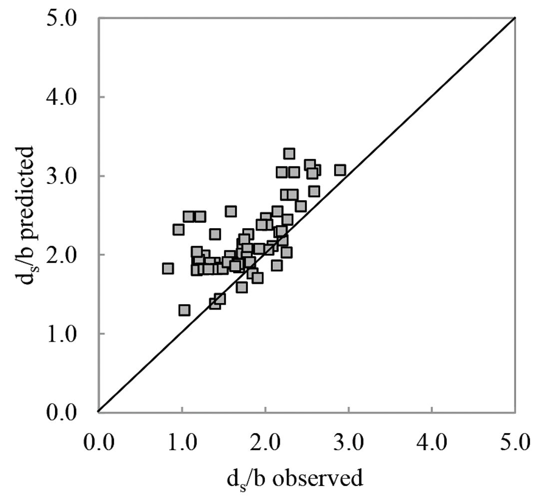

Figure 6. Comparison of observed values of ds/b around wide piers with those predicted using Equation [1] and Equation [2]

CONCLUSION

In conclusion, the temporal and scour hole development of local scour depth with new laboratory data is demonstrated for the flow intensity $U/U_c = 0.95$. The effects of local scour depth at wide piers on scour hole development and sediment coarseness were presented. It was found that the relative scour depth d_{se}/b decreased with increasing values of sediment coarseness

b/d_{50}. Two continuous upper envelope equations for pier scour depth as a function of b/d_{50} were developed according to the value of b/d_{50} (≤ 37 and > 37). It was proved that for large values of b/d50, the values of dse/b become reduced., and this was consistent with results of experiments using very large flumes as well as findings by previous researchers. Experimental results and analysis of the effects of pier width and bed sediment size on scour depth validate the theory of wide piers for the most part. However, the results of the present study are limited to clear-water conditions, steady flow, non-cohesive sediments, and subcritical flow conditions. An important practical limitation of laboratory experiments on pier configuration is flume width; the size of the flume is not wide enough to facilitate scour experiments for large values of b.

ACKNOWLEDGEMENTS

The financial support via the Research University Grant Scheme (RUGS), University Putra Malaysia (Grant No. 05-01-10-0904RU), for this project is acknowledged. The experiments were conducted at the Hydraulic Laboratory in the National Hydraulic Research Institute of Malaysia (NAHRIM).

REFERENCES

Arneson, L. A., Zevenbergen, L. W., Lagasse, P. F., & Clopper, P. E. (2012). Evaluating scour at bridges (4th Ed.). *Hydraulic Engineering Circular No. 18* (HEC-18). Federal Highway Administration, Washington, DC.

Ettema, R., (1980). *Scour around bridge piers.* Report No. 216, University of Auckland, Auckland, New Zealand.

Ettema, R., (1980). *Scour around bridge piers.* Report No. 216, University of Auckland, Auckland, New Zealand.

Ettema, R., Kirkil, G., & Muste, M. (2006). Similitude of large-scale turbulence in experiments on local scour at cylinders. *Journal of Hydraulic Engineering, 132*(1), 33-40.

Johnson, P. A., & Torrico, E. F. (1994). Scour around wide piers in shallow water. *Transportation Research Record,* (1471), 66-70.

Johnson, P. A. (1999). Scour at Wide Piers Relative to Flow Depth, Stream Stability and Scour at Highway Bridges. In E. V. Richardson & P. F. Lagasse (Eds.), *Compendium of ASCE Conference Papers* (pp. 280–287).

Jones, J., & Sheppard, D. (2000). *Scour at wide bridge pier* (pp. 1-10). Federal Highway Administration, Turner-Fairbank Highway Research Center, McLean, Virginia.

Junliang, T., & Xiong, Y. (2014). Flow and Scour Patterns around Bridge Piers with Different Configurations: Insights from CFD Simulations. In *Geo-Congress 2014 Technical Papers: Geo-characterization and Modeling for Sustainability* (pp. 2655-2664). ASCE.

Kirkil, G., Constantinescu, S. G., & Ettema, R., (2008). Coherent structures in the flow field around a circular cylinder with scour hole. *Journal of Hydraulic Engineering, 134*(5), 572–587.

Lança, R. M., Fael, C. S., Maia, R. J., Pêgo, J. P., & Cardoso, A. H. (2013). Clear-water scour at comparatively large cylindrical piers. *Journal of Hydraulic Engineering, 139*(11), 1117-1125.

Lee, S. O., & Sturm, T. W. (2009). Effect of sediment size scaling on physical modeling of bridge pier scour. *Journal of Hydraulic Engineering, 135*(10), 793-802.

Melville, B. W., & Coleman, S. E., (2000). *Bridge Scour*. United States of America, USA: Water Resources Publications.

Melville, B.W., (1975). *Local scour at bridge sites*. Report No.117. School of Engineering, University of Auckland, New Zealand.

Melville, B. W. (2008). The physics of Local Scour at Bridge Piers. In *Fourth International Conference on Scour and Erosion* (pp. 28-38). Tokyo.

Nicolet, G. (1971). *Deformation des lits alluvionaires affouillements autor des piles se ponts cylindriques*. Report No. HC 043 684. Laboratoire National d'Hydraulique, Chatou, France.

Sheppard, D. M., Huseyin, D., & Melville, B. W. (2011). *Scour at wide piers and long skewed piers*. Report (National Cooperative Highway Research Program); 682. Washington, D.C.: Transportation Research Board.

Sheppard, D. M., Melville, B., & Demir, H. (2013). Evaluation of existing equations for local scour at bridge piers. *Journal of Hydraulic Engineering, 140*(1), 14-23.

Sheppard, D. M., & Miller, J. W. (2006). Live-bed local pier scour experiments. *Journal of Hydraulic Engineering, 132*(7), 635-642.

Sheppard, D. M., Odeh, M., & Glasser, T. (2004). Large scale clear-water local pier scour experiments. *Journal of Hydraulic Engineering, 130*(10), 957-963.